AGU PUBLICATIONS

Geophysical Research Letters

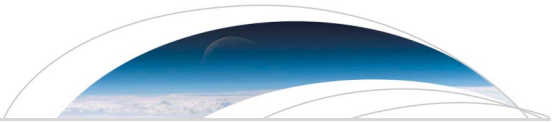

RESEARCH LETTER

10.1002/2014GL060649

Key Points:
- Water solubility of organic vapors is correlated to their vapor pressures
- Henry's law constants as a function of volatility are provided for 3-D models
- Dry/wet deposition of condensable organic gases mediates atmospheric SOA loss

Supporting Information:
- Readme
- Tables S1 and S2
- Figures S1 and S2
- Figures S3 and S4
- Figure S5
- Figure S6
- Figure S7

Correspondence to:
A. Hodzic,
alma@ucar.edu

Citation:
Hodzic, A., B. Aumont, C. Knote, J. Lee-Taylor, S. Madronich, and G. Tyndall (2014), Volatility dependence of Henry's law constants of condensable organics: Application to estimate depositional loss of secondary organic aerosols, *Geophys. Res. Lett.*, *41*, 4795–4804, doi:10.1002/2014GL060649.

Received 27 MAY 2014
Accepted 13 JUN 2014
Accepted article online 18 JUN 2014
Published online 15 JUL 2014

Volatility dependence of Henry's law constants of condensable organics: Application to estimate depositional loss of secondary organic aerosols

A. Hodzic[1], B. Aumont[2], C. Knote[1], J. Lee-Taylor[1], S. Madronich[1], and G. Tyndall[1]

[1]NCAR, Boulder, Colorado, USA, [2]LISA UMR CNRS 7583, Université Paris Est Créteil et Université Paris Diderot, Créteil, France

Abstract The water solubility of oxidation intermediates of volatile organic compounds that can condense to form secondary organic aerosol (SOA) is largely unconstrained in current chemistry-climate models. We apply the Generator of Explicit Chemistry and Kinetics of Organics in the Atmosphere to calculate Henry's law constants for these intermediate species. Results show a strong negative correlation between Henry's law constants and saturation vapor pressures. Details depend on precursor species, extent of photochemical processing, and NO_x levels. Henry's law constants as a function of volatility are made available over a wide range of vapor pressures for use in 3-D models. In an application using the Weather Research and Forecasting model coupled with Chemistry (WRF-Chem) over the U.S. in summer, we find that dry (and wet) deposition of condensable organic vapors leads to major reductions in SOA, decreasing surface concentrations by ~50% (10%) for biogenic and ~40% (6%) for short chain anthropogenic precursors under the considered volatility conditions.

1. Introduction

The fate of volatile organic compounds (VOCs) emitted into the atmosphere by anthropogenic activities and biogenic sources is currently not well understood nor captured in chemistry-climate models [*Hallquist et al.*, 2009]. Directly emitted VOCs undergo a number of oxidation reactions in the atmosphere until they are completely degraded to CO and CO_2, permanently condensed into particles and cloud droplets, or deposited to the ground. The lifetime of these molecules in the atmosphere depends strongly not only on chemical and atmospheric conditions but also on their thermodynamic properties such as volatility or solubility in water. The volatility describes the ability of oxidized VOCs to partition into the particle phase according to Raoult's law to form secondary organic aerosols (SOA) [*Donahue et al.*, 2006], whereas the solubility describes their ability to dissolve into aqueous particles or cloud droplets according to Henry's law or to deposit to the ground [*Ervens et al.*, 2011]. Modeling of these properties for oxidation products of various types of VOCs and how they evolve with chemical aging is key to accurately predicting the atmospheric SOA burden. It is, however, challenging given the large number of intermediate compounds involved, which span several orders of magnitude in volatility and water solubility (Figure 1).

Field measurements and explicit modeling suggest that contributors to organic aerosols (OA) are generally less volatile and more water soluble than their parent compounds due to continuous chemical processing in the atmosphere [e.g., *Zhang et al.*, 2007; *Mouchel-Vallon et al.*, 2013; *Hodzic et al.*, 2013]. To account for this decrease in volatility, the most recent SOA formation mechanisms were updated to include multigenerational oxidation of VOCs as a function of their volatility [*Robinson et al.*, 2007, *Lane et al.*, 2008]. The most common approach, known as the volatility basis set (VBS), allows parameterizing a large fraction of oxygenated OA present in the atmosphere using a finite number of volatility surrogates and has been implemented in regional and global 3-D models [e.g., *Jo et al.*, 2013, *Hodzic et al.*, 2010]. The increase in water solubility with chemical processing is on the other hand parameterized in a very crude way in current 3-D models and only for organic particles (rarely organic gases). Most chemistry climate models simply apply a first order conversion rate of hydrophobic to hydrophilic OA with the characteristic time constant of 0.7–1.2 days [*Kanakidou et al.*, 2005]. The solubility of condensable organic vapors is rarely considered in models, and when it is included, an effective Henry's law constant of 10^5 M atm^{-1} is generally used used for all species [*Pye and Seinfeld*, 2010; *Jo et al.*, 2013]. In this paper, we explicitly describe the change in solubility of organic material that occurs with chemical processing. For that purpose, we apply the explicit chemistry model GECKO-A (Generator of Explicit Chemistry and Kinetics of Organics in the Atmosphere) [*Aumont et al.*, 2005] to calculate the water solubility of

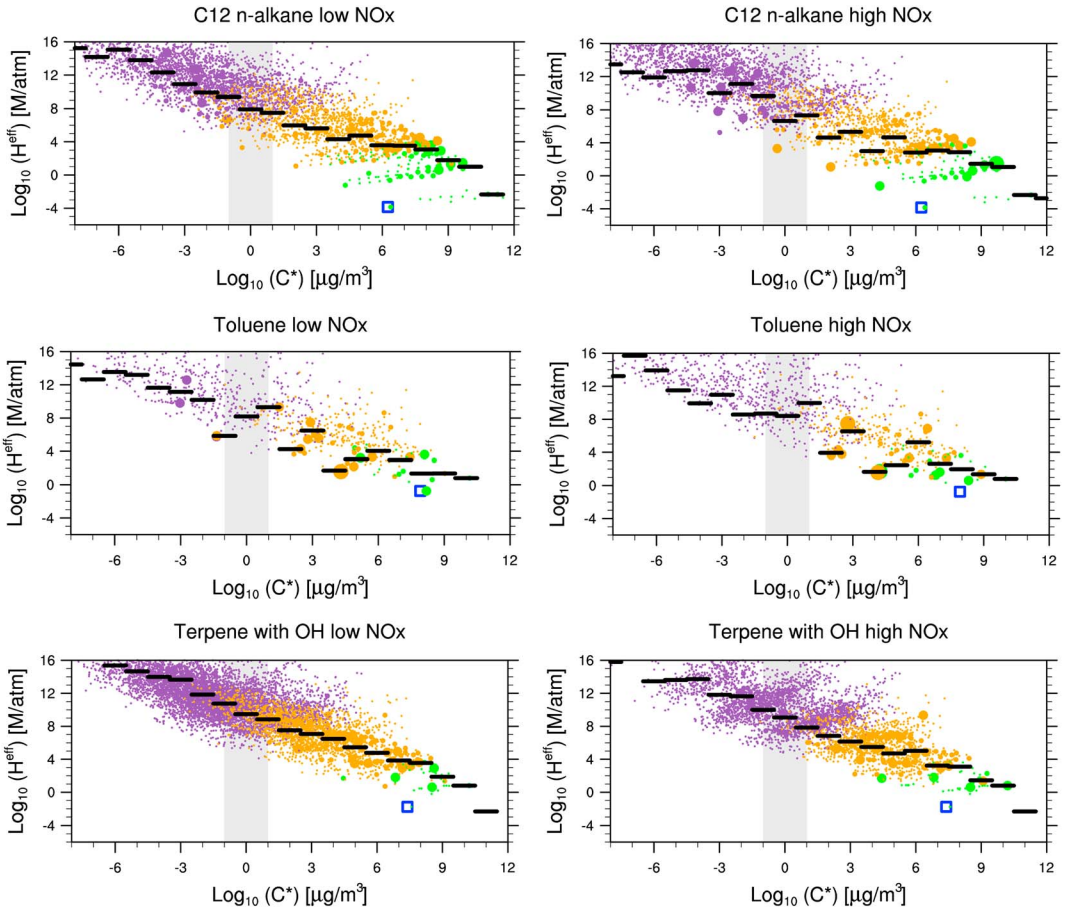

Figure 1. Effective Henry's law constant of molecules as a function of their volatility. Black lines indicate the mean mass weighted Henry's law constant in each volatility bin. Oxidation products from C_{12} n-alkane, toluene, and terpene (a mixture of α-pinene, β-pinene, and limonene) precursors are shown at the maximum of SOA production in the run. The size of each circle indicates the relative contribution of the specific compound to the total organic mass, whereas the color indicates the number of functional groups (green 0–1 functional groups, orange 2–3 functional groups, and purple >4 functional groups). Gray shading indicates the gas-particle partitioning zone for the current mixture: A species left (right) of the gray region has >90% of the mass in the particle (gas). Isomers with the same C^* and H are lumped together, and species with total concentrations of less than 10^2 molecules cm^{-3} are not considered. The precursor is indicated by a blue square.

oxidation products of major anthropogenic and biogenic VOCs involved in SOA formation and study how it evolves with chemical processing, vapor pressures, and NO_x levels. The objective is to derive a simplified parameterization of solubility as a function of vapor pressures that can be used within the VBS framework in 3-D models to quantify the role of semivolatile organic compounds (SVOCs) in SOA removal.

Inaccurately representing the solubility of semivolatile organic gases (SVOC) and particles in 3-D models currently leads to yet unquantified errors in estimated OA removal, and therefore OA lifetime and burden in the atmosphere. To our knowledge only a few studies have investigated the importance of SVOC depositional removal on OA concentrations. *Hodzic et al*. [2013] explicitly calculated dry deposition of anthropogenic organic vapors in an urban plume typical of a megacity using a Lagrangian box model and showed that such deposition is relatively small (<15%) because soluble gases preferentially partition to the particle phase which does not deposit efficiently. *Bessagnet et al*. [2010] found a larger impact over Europe on their predicted SOA, which was formed 95% from biogenic precursors. By assigning an ad hoc solubility parameter to lumped oxidation products of VOC precursors in their 3-D model, Bessagnet et al. estimated that dry deposition removes on average 30% of the SOA mass, and up to 50% in some forested regions. Here we will apply the parameterization developed in this study within a 3-D model to quantify the regional importance of dry and wet removal of organic vapors for SOA concentrations.

2. Modeling Approach

2.1. GECKO-A Chemical Mechanism and Simulation Conditions

The GECKO-A model [*Aumont et al*., 2005] was applied to generate VOC oxidation mechanisms for individual precursors including isoprene, α-pinene, β-pinene, limonene, toluene, p-, m-, o-xylene, $C_{8,12,18,22}$-alkanes, and C_{12}-alkenes. The chemical schemes are created using a prescribed set of rules determining reaction pathways and rate coefficients, based on laboratory kinetic data, and structure-activity relationships. Instantaneous equilibrium is assumed [*Pankow*, 1994] for gas-particle partitioning following Raoult's law, and using the *Nannoolal et al*. [2008] method to estimate the saturation vapor pressure for nonradical species. The fraction that is partitioned to the aerosol phase can be determined as follows: $F_{\mathrm{aerosol},i} = \left(1 + C_i^* / C_{\mathrm{OA}}\right)^{-1}$ where C_{OA} is the total organic aerosol mass concentration ($\mu g/m^3$) and C_i^* is an effective saturation mass concentration ($\mu g/m^3$) that is used in the VBS parameterization [*Donahue et al*., 2006]. Heterogeneous or aqueous phase reactions are not considered.

The concentration of a gas dissolved in a liquid is proportional to its partial pressure above that liquid and Henry's law constant (H, M/atm). Here H refers by default to the effective Henry's law constant, which includes the hydration process. H depends mainly on the type and number of functional groups that are attached to the carbon chain. Values of H for organic compounds are estimated at 298 K using the GROup contribution Method for Henry's law Estimate (GROMHE) [*Raventos-Duran et al*., 2010] based on currently available data for 488 organic compounds covering a wide range of functional groups. A multiple linear regression based on functional groups and the number of C, H atoms is applied to derive H for hundreds of thousands of organic species that are simulated by GECKO-A. *Raventos-Duran et al*. [2010] showed that H values for hydrocarbon and monofunctional compounds were well predicted and that the reliability of the predicted values decreases for larger H values. The root-mean-square error for species with $H > 10^3$ M/atm obtained with GROMHE was half (0.53 log units) of that found with the HENRYWIN [*Meylan and Howard*, 2000] and SPARC methods [*Hilal et al*., 2008] (~1 log unit).

Similar to *Aumont et al*. [2012], in this study simulations are performed in a box model with prescribed conditions aimed to be representative of ambient conditions. Temperature is set to 298 K; photolysis frequencies are calculated for midlatitudes at a solar zenith angle of 30°; NO_x levels are set to 0.1 ppb for low-NO_x and 10 ppb for high-NO_x conditions; OH is kept constant at 2×10^6 molecules/cm^3; and ozone is set at 40 ppb, CO at 80 ppb, CH_4 at 1.68 ppm, and preexisting aerosols used for partitioning are set to a typical background of 1 $\mu g/m^3$. The NO_2/NO ratio is internally calculated by GECKO, and the contributions of peroxyacetylnitrate-like compounds to SOA and their dependence on the NO_2/NO ratio is explicitly treated. The initial concentration of the precursor is fixed to a very low value of 1 ppt so that the amount of aerosol produced from the given precursor is negligible compared to preexisting C_{OA} and that the aerosol yield is independent of initial concentrations of the precursor as already shown in *Aumont et al*. [2012]. By treating the presence of a given hydrocarbon as a perturbation on the "background atmosphere" which contains CO and CH_4, we do not produce any large variations in the levels of oxidants such as OH, HO_2, and O_3. Since the potential for the production of SOA is typically thought to be additive, we can thus build up a representative model of SOA formation. The resulting ratios of NO to HO_2, relevant for peroxy radical (RO_2) chemistry, are typical of rural (low NO_x) and urban (high NO_x) conditions. We calculated in GECKO-A the corresponding branching ratio of RO_2 reacting with NO versus HO_2 as used in 3-D models [*Lane et al*., 2008] and found that it is equal to 0.6 at low-NO_x and to 0.99 at high-NO_x conditions and comparable to typical values predicted over the U.S. [*Pye et al*., 2010].

2.2. Regional WRF-Chem Simulations

Weather Research and Forecasting model coupled with Chemistry (WRF-Chem) (v3.5) was applied over the continental U.S. at 36 km resolution during summer (July to September) 2010 using the extended gas-phase chemistry from MOZART-4 (Model for Ozone and Related Chemical Tracers version 4 [*Emmons et al*., 2010; *Knote et al*., 2014a]) and MOSAIC sectional aerosols [*Zaveri et al*., 2008]. A VBS with five bins (C* of 0.001, 1, 10, 100, and 1000 $\mu g/m^3$) has been added similar to *Knote et al*. [2014b] to describe SOA formation from the oxidation of biogenic and anthropogenic precursors following the NO_x-dependent yields from *Lane et al*. [2008]. These vapors age through reaction with OH ($k_{\mathrm{OH}} = 10^{-11}$ cm^3 $molecules^{-1}$ s^{-1}, as in *Murphy and*

Pandis [2009]), gaining 7.5% mass through oxygen addition and moving down one volatility bin. The volatility characteristics of the VBS parameterization are reviewed in the supporting information. Equilibrium partitioning between gas and aerosol phases follows *Pankow* [1994]. Primary OA is directly emitted and considered to be inert, residing permanently in the aerosol phase. Dry deposition is calculated using a resistance analogy based on *Wesely* [1989] that opposes three resistances to the uptake of gas species including the aerodynamic resistance (*R*a), the resistance associated with transport through the quasi-laminar layer in contact with the canopy (*R*b), and the surface resistance (*R*c). *R*a depends only on meteorological conditions, while *R*b also depends on the molecular diffusivity of the gas. The surface resistance is a function of the water solubility (Henry's law constant) of the gas through the calculation of component resistances including the mesophyll and the leaf cuticular resistances, the resistance of exposed surfaces in the lower canopy, and the ground surface resistance. A more detailed description of these dependences can be found in the supporting information. SVOCs are considered as unreactive gases and the reactivity factor in the calculation of the surface resistance is set to zero as commonly assumed. Wet deposition in WRF-Chem is a combination of resolved [*Neu and Prather*, 2012] and convective washout [*Grell and Dévényi*, 2002]. In both schemes, gases partition into droplets according to their *H* before being deposited. In the base model configuration, removal is represented by dry and wet depositions of all aerosols and gases except SVOCs for which *H* values were not previously available. In the sensitivity studies performed here we added dry and wet depositions of SVOCs considering the removal in each volatility bin according to *H* values determined from GECKO-A.

3. Results and Discussion

3.1. Parameterizing Water Solubility of Oxidized Species as a Function of Their Volatility

The results of the GECKO-A simulations for individual precursors are plotted in a 2-D volatility-solubility grid (Figures 1 and S3 in the supporting information), where volatility is represented by saturation mass concentrations C^* ($\mu g/m^3$), calculated from the saturation vapor pressures of all nonradical species, and water solubility is represented by the effective Henry's law constant. We have reported *H* values at the maximum of SOA formation as is typically done for SOA yields. Figure 1 shows the properties of the oxidation products of C_{12} *n*-alkane, toluene, and terpenes. It is clearly apparent that the chemically processed species are more soluble and generally less volatile than their parent compounds. Water solubility is increased by several orders of magnitude with increasing number of functional groups and is inversely associated with volatility. Typically, it increases from 10^{-4}–10^{-1} M/atm for parent species, to 10^{-1}–10^{4} M/atm for organic molecules with one functional group, to 10^{2}–10^{9} M/atm with two or three functional groups and exceeds 10^{6} M/atm for highly functionalized species which are found mostly in the particle phase. Compounds that are not partitioned to the particle phase and have high solubility ($H > 10^{5}$ M/atm) are likely to partition to cloud droplets [*Seinfeld and Pandis*, 2006] or to dry deposit with significant deposition velocities ($Vd > 1$ cm/s) [*Hodzic et al.*, 2013]. Line-like features that are visible in Figure 1 for *n*-alkanes where *H* increases by 1–2 orders of magnitude, but C^* increases by up to 7, correspond to carbon loss by fragmentation. Similar dependencies between *H* and C^* are observed for products of major biogenic and anthropogenic precursors (α-pinene, β-pinene, limonene, toluene, p-, m-, o-xylene, $C_{8,\ 12,\ 18,\ 22}$-alkanes, and C_{12}-alkenes (Figure S3)), and relatively small differences are found between low- and high-NO_x cases as discussed below.

To facilitate the parameterization of water solubility of organics within a 3-D model, *H* values predicted by GECKO-A for each molecule have been averaged over selected volatility bins spaced by unity in log space for some of the major SOA precursors as used in the SAPRC gas phase mechanism [*Carter*, 2010] and summarized in Figure 2 and Table S1. The average *H* is weighted by the relative mass contribution of individual molecules in each bin. The variability associated with the bin-averaged *H* typically varies by 1 to 2 orders of magnitude and exceeds 3 orders of magnitude for larger *n*-alkane species. Figure 2 shows a quasi-linear dependence of $\log_{10}(H)$ with $\log_{10}(C^*)$ for all precursors, with individual correlation coefficients above 0.8 (Table 1). The slope of the linear regression varies between -0.5 and -0.9, whereas the intercept (i.e., $C^* = 1\ \mu g/m^3$) is typically around $10^{6.5}$ M/atm for products of long-chain n-alkanes, between 10^{8} and 10^{9} M/atm for all other considered anthropogenic species, i.e., light aromatics, short-chain *n*-alkenes, and olefins and above 10^{9} M/atm for biogenic products. These results suggest that the oxidation products of biogenic precursors are typically more soluble than those of anthropogenic precursors (the intercept for

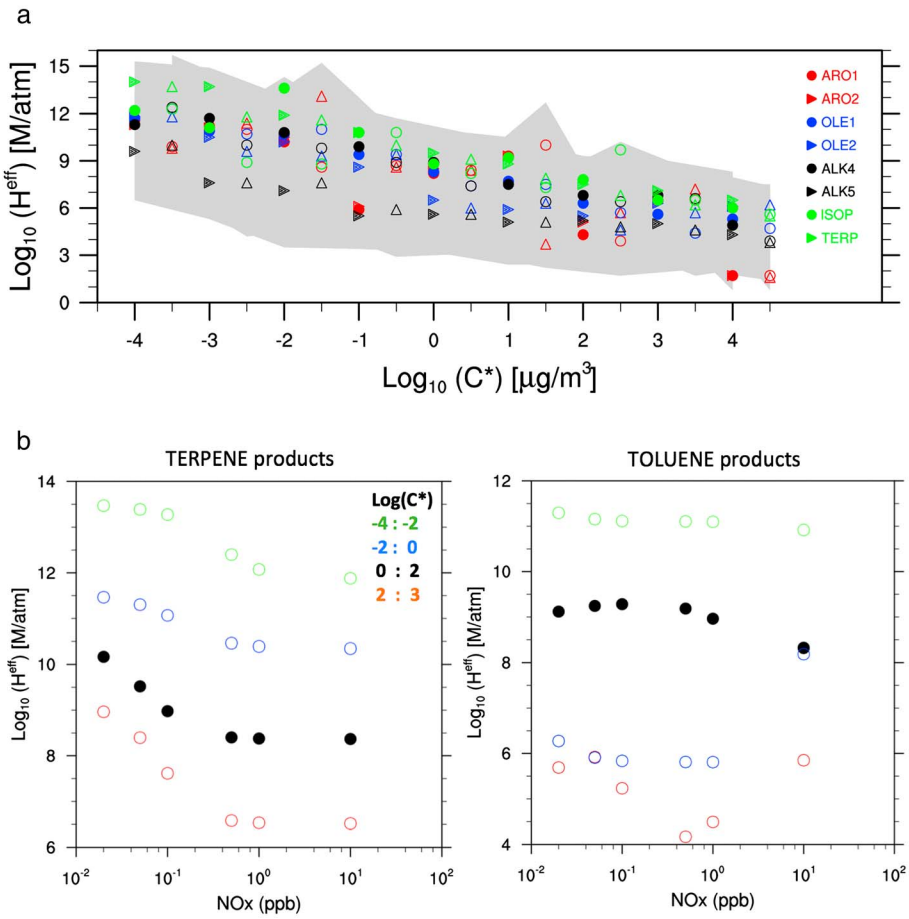

Figure 2. (a) Henry's law constant for oxidation products of major biogenic and anthropogenic SOA precursors shown as a function of their volatility. Full circle and triangle symbols indicate low NO_x (0.1 ppb) whereas empty symbols represent high-NO_x (10 ppb) conditions. Gray shading indicates the 1 sigma variability in log units associated with the averaging over each volatility bin. (b) Dependence of H values on NO_x levels is shown for products of terpene and toluene.

Table 1. Effective Henry's Law Constant H (M/atm) at 298 K[a] Expressed as a Function of Volatility C^* (µg/m^3) and NO_x Levels Using Linear Regression in Log Space: $\log_{10}(H) = a \times \log_{10}(C^*) + b$[b]

	Low NO_x (0.1 ppb)			High NO_x (10 ppb)		
Precursor[c]	Slope (a)	Intercept (b)	r^2	Slope (a)	Intercept (b)	r^2
ARO1	−0.85	8.04	0.88	−0.79	7.91	0.85
ARO2	−0.78	8.17	0.87	−0.84	7.89	0.82
OLE1	−0.81	8.77	0.98	−0.82	8.32	0.96
OLE2	−0.75	8.12	0.95	−0.77	7.90	0.89
ALK4	−0.86	8.72	0.98	−0.84	8.09	0.95
ALK5	−0.51	6.43	0.93	−0.58	6.46	0.92
ISOP	−0.85	9.39	0.96	−0.77	8.46	0.92
TERP	−0.90	10.05	0.99	−0.84	9.22	0.98

[a] H can be derived for a different temperature T (K) following the van't Hoff equation: $H_T = H_{298} \times \exp\left[\frac{\Delta H_{solv}}{R}\left[\frac{1}{T} - \frac{1}{298}\right]\right]$ where ΔH_{solv} is the desolvation enthalpy set to 50 kJ/mol [*Raventos-Duran et al.*, 2010] and R is the gas constant.
[b] ARO1 is representative of toluene; ARO2 of xylenes; OLE1 of C_{12} internal olefins; OLE2 of C_{12} external olefins; ALK4 of C_8 *n*-alkane; ALK5 of C_{18} *n*-alkane; and TERP of a mixture of α-pinene, β-pinene, and limonene.
[c] Reported H values correspond to the maximum of SOA formation.

terpenes is larger by 2 orders of magnitude than that of toluene) as also illustrated in Figure 2. The average H calculated over the entire distribution of oxidation products of terpenes is larger by 3 orders of magnitude than that of toluene products (not shown here). *Couvidat and Seigneur* [2011] have also reported elevated H values (up to 8.9×10^{10} M/atm) for oxidation products of isoprene.

The elevated $\log_{10}(H)$ intercept values indicate that gas species with $C^* = 1\ \mu g/m^3$ and below are likely to be dissolved into cloud droplets. The aqueous fraction that is in thermodynamic equilibrium with the gas phase can be calculated as $X_{aq} = \left(1 + \frac{1}{H \times R \times T \times LWC}\right)^{-1}$ where H is the effective Henry's law constant (M/atm), R the ideal gas constant ($R = 0.082$ L atm K^{-1} mol^{-1}), T is the temperature (K), LWC the liquid water content (cm^3 liquid water per cm^3 air). For typical cloud LWC of 10^{-7} cm^3 liquid water per cm^3 air [*Seinfeld and Pandis*, 2006], the dissolved fraction is ~70% for $H = 10^6$ M/atm and ~96% for $H = 10^7$ M/atm.

For highly functionalized species GECKO-A predicts large H values up to 10^{16} M/atm. Such high values ($>10^{12}$ M/atm) have recently been derived for polyols (compounds with two or more hydroxyl groups) using a different methodology from the one used in this study [*Compernolle and Müller*, 2014]. Uncertainties associated with the GROMHE estimates in that range of values are expected to be significant, because the extrapolation is performed beyond experimentally measured values (typically up to 10^9 M/atm for oxalic acid [*Raventos-Duran et al.*, 2010]). However, these uncertainties are not of concern for our study as under most atmospheric conditions, compounds having $H > 10^{12}$ M/atm are expected to be almost exclusively in the aqueous phase and their gas phase concentrations can be considered as negligible [*Mouchel-Vallon et al.*, 2013]. In addition, for species with high H (typically $H > 10^7$ M/atm), deposition is no longer dependent on the surface resistance but is limited by the aerodynamic resistance and the transport through the laminar layer [*Hodzic et al.*, 2013], and uncertainties in H values above this threshold are not expected to impact our conclusions (see Figure S5).

Distribution and properties of oxidation products of anthropogenic and biogenic VOCs are NO_x dependent [*Hallquist et al.*, 2009]. At low NO_x, hydroperoxides and carbonyls are formed, while at high-NO_x peroxynitrates and nitrates dominate. Dependence of H on NO_x levels is investigated by comparing H values obtained at 0.1 ppb and 10 ppb NO_x for all precursors considered in this study (Figure 2 and Table 1). Table 1 shows that the difference in slope and intercept for $\log_{10}(H)$ values between the two NO_x cases is less than 10% in a log-log space for all precursor species (except for ALK5 for which the slope is changed by 14%). An increase in H up to an order of magnitude in the intercept is generally observed for lower NO_x, indicating that the products formed are typically more water soluble. To calculate the SOA production at the ambient NO_x levels, 3-D models typically apply a linear interpolation between low- and high-NO_x SOA yields. Figure 2b indicates that linear interpolation might not be suitable between H values reported for 0.1 and 10 ppb. For products of terpene, H stays remarkably constant for NO_x between 0.3 and 10 ppb, whereas it increases sharply (by about an order of magnitude) for NO_x lower than 0.3. For products of toluene, the H dependency on NO_x levels changes with C^*. Modeled H values as a function of NO_x for individual precursors presented in this paper can be obtained upon request from the authors.

3.2. Effect of Dry and Wet Depositions of Condensable Organic Vapors on SOA

The advantage of providing H as a function of volatility for condensable organic compounds is that it can be easily linked with the VBS parameterizations used to describe the SOA formation in 3-D models. Here we implemented the coefficients reported in Table 1 for low-NO_x values into the WRF-Chem model to quantify the importance of the removal of condensable organic vapors on SOA regional concentrations. We used low-NO_x values as they are more representative of the NO_x levels found over the continental U.S. away from urban areas as suggested by the WRF-Chem simulated median NO_x concentrations in the boundary layer of ~200 ppt during summer (not shown here). Results over the continental U.S. are shown in Figure 3 for the summer of 2010.

The predicted averaged SOA concentrations show a strong west-east gradient as already reported by previous studies [e.g., *Fann et al.*, 2012]. Anthropogenic SOA ranges from 0.5 to 1 $\mu g/m^3$ background levels to ~3 $\mu g/m^3$ concentrations on the East Coast and the southeast U.S. Biogenic SOA peaks at 5–6 $\mu g/m^3$ over the southeast U.S., while background levels are ~1 $\mu g/m^3$. As expected given higher Henry's law constants, the dry deposition removal relative to the initial SOA concentrations is larger for biogenic precursors as it

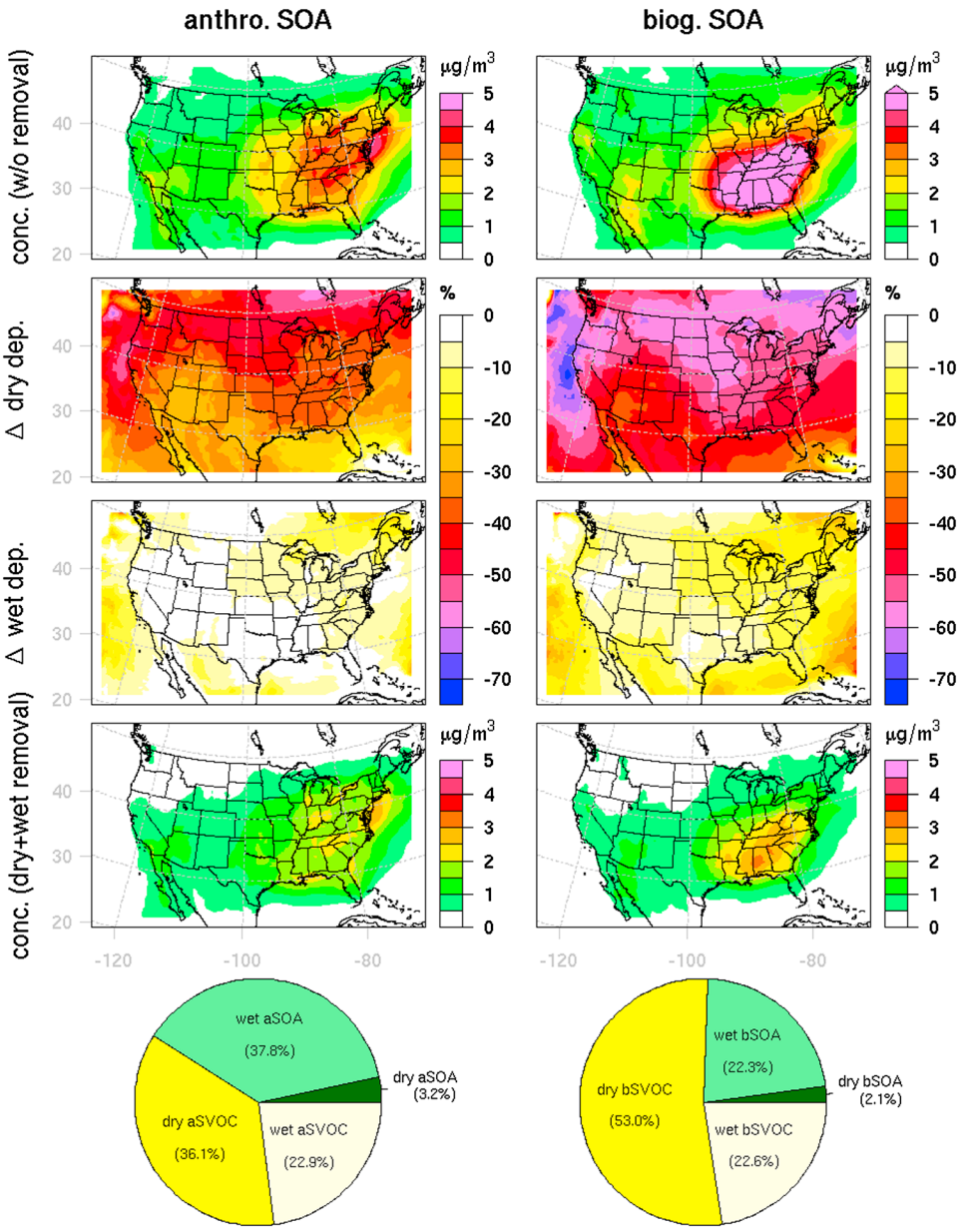

Figure 3. Anthropogenic and biogenic SOA surface concentrations over the continental U.S. as predicted by WRF-Chem during summer (July to September) 2010. (first row) The results of the default WRF-Chem simulation without deposition of semivolatile organic vapors (SVOCs); (fourth row) the results of the sensitivity simulation that includes dry and wet removal of both SVOCs and SOA. (second and third rows) Percent change in SOA surface concentrations due to dry and wet deposition of SVOCs. Pie charts show the relative contribution of dry and wet deposition to the total deposited mass of SOA and SVOCs during the considered summer period.

decreases the SOA concentrations by 40–60%, compared to 30–40% for anthropogenic species. The largest dry deposition loss of SVOCs occurred over forested regions especially over the southeast U.S. (see Figure S7), although the resulting decrease in SOA concentrations is spatially spread out. The relative SOA loss by wet deposition of SVOCs is smaller during the chosen time period with a ~10–15% decrease for biogenic and 5–10% for anthropogenic SOA. For biogenics, our results are consistent with *Bessagnet et al.* [2010] who reported a 30–50% sink for biogenic SOA over Europe due to dry deposition of condensable organic vapors. However, our results indicate a factor of two larger impact of dry deposition of SVOCs on anthropogenic SOA compared to the idealized urban plume (Lagrangian) study reported by *Hodzic et al.* [2013], likely due to a combination of factors including the representation of the boundary layer mixing and height, different

emission profiles, or vapor pressure scheme (Hodzic et al. used the less volatile scheme of *Myrdal and Yalkowsky* [1997], and here we use the updated and more accurate scheme of *Nannoolal et al*. [2008]). The comparison of the predicted surface organic carbon with the IMPROVE network data during summer 2010 (Figure S6) shows an improved agreement with observations when dry and wet deposition of SVOCs is considered. The normalized mean bias of 32% found in the default simulation is reduced to −14% when SVOC deposition is included, and the correlation coefficient is slightly improved from 0.42 to 0.46. However, one should be careful when interpreting this relative improvement in surface OC predictions as the production and properties of SOA are still highly uncertain.

Our results suggest that SOA loss is mediated by SVOCs instead of occurring as currently believed almost uniquely (~85%) through the wet scavenging of SOA particles as reviewed by *Kanakidou et al*. [2005]. The pie charts in Figure 3 show the relative importance of dry and wet removal of organic gases and particles. The loss of SOA and condensable vapors is dominated by dry (36–53%) and wet (~23%) removal of SVOCs, with a smaller contribution of wet (22–38%) and dry (2–3%) deposition of SOA particles. For biogenic compounds, dry removal of SVOCs is the largest loss (53%), whereas for anthropogenic species, dry removal of SVOCs and wet scavenging of SOA are comparable (~36–39%). Given the relative importance of dry removal of SVOCs, the results also suggest that the predicted mass of secondary organic species is less dependent on the accuracy of cloud predictions. The uncertainties related to cloud handling in the model are not expected to impact our conclusions as the model was shown to reasonably reproduce precipitation and wet deposition of inorganic ions during the period of interest [*Knote et al*., 2014b]. It should also be noted that in this study SVOCs were treated as unreactive gases as their reactivity is not well known from measurements. *Karl et al*. [2010] suggested that oxygenated VOCs (e.g., products of isoprene) could be as reactive as ozone, leading to a much larger loss of these species to vegetation, which would imply that our estimates of dry removal of SVOCs could be underpredicted.

As SVOCs that have not yet partitioned to the particle phase (or have evaporated) play the major role in the SOA reduction, the results are expected to be sensitive to the volatility of the SOA formation mechanism, which is still highly unconstrained. *Hodzic et al*. [2013] showed that up to 60% overestimation of the dry deposition of anthropogenic SOA could result from artificially assuming (as an extreme upper estimate) SVOCs to be totally volatile in the GECKO-A model. The sensitivity of our results to the volatility assumptions and the VBS scheme details are discussed in the supporting information (Figures S1 and S2) and will be further investigated in a separate study [*Knote et al*., 2014b]. Briefly, the five-bin VBS SOA formation scheme considered in this study was made less volatile by adding an additional bin to the four-bin VBS of *Lane et al*. [2008] to allow the formation of nonvolatile SOA and limit the effect of SVOC deposition (the difference is ~20%, supporting information). The considered aging rate constant ($k_{OH} = 10^{-11}$ cm^3 molecules^{-1} s^{-1}) is within the uncertainty of previously suggested values (ranging from 4×10^{-12} to 4×10^{-11} cm^3 molecules^{-1} s^{-1}, *Lane et al*., 2008). If a four times faster ageing of SVOCs is considered, the influence of the SVOC removal on SOA surface concentrations is still considerable 23% (anthropogenic) and 39% (biogenic) [*Knote et al*., 2014b]. It should also be noted that oligomerization reactions that can lower the volatility of organic compounds and prevent their evaporation are not included in this study [e.g., *Tolocka et al*., 2004; *Vaden et al*., 2011]. As sources and processes controlling SOA formation are still highly uncertain and under investigation [*Hallquist et al*., 2009], our results are valid for the considered (or similar) volatility conditions.

4. Conclusions

We studied and parameterized the evolution of the Henry's law constants (water solubility) of condensable organic vapors as a function of their saturating mass concentration (volatility) using explicit chemical modeling of oxidation products of major biogenic and anthropogenic SOA precursors. This parameterization was implemented into the regional chemistry transport model WRF-Chem to evaluate the importance of the dry and wet removal of condensable vapors on regional SOA concentrations. Our main findings are the following:

1. A multiday atmospheric processing of biogenic and anthropogenic VOCs leads to the formation of highly functionalized and water soluble organic vapors. We have shown that their water solubility as represented by the effective Henry's law constants can be parameterized as a simple function of volatility, and have

provided Henry's law constants for the volatility basis set framework used in 3-D models for major SOA precursors and for low-NO_x (0.1 ppb) and high-NO_x (10 ppb) levels. The provided parameterization can be easily used in 3-D models to simulate dissolution of SVOCs into aqueous particles, cloud droplets, and plant water.

2. Regional simulations suggest that removal of tropospheric SOA is mainly happening through dry and wet deposition of condensable organic vapors (60–75%) and not the direct scavenging of SOA particles. Model results over the U.S. during summer suggest up to 50% reduction in surface SOA by dry deposition for biogenic vapors (compared to ~40% reduction for products of short-chain anthropogenic precursors), because of the higher Henry's constants associated with biogenic compounds. The impact of wet deposition of SVOCs on SOA is 4 times lower (~6–11%).

Our results on the importance of SVOCs removal on SOA levels are valid under current volatility assumptions of the SOA formation mechanisms, which are the ones most commonly used in chemistry-climate models. The comparison with OA surface data indicates that model results are consistent with ambient measurements when the removal of SVOCs is considered. These measurements by themselves, however, do not provide a sufficient constraint on removal mechanisms. Measurements of water solubility and deposition fluxes of condensable organics would be extremely valuable to further constrain the GECKO-A solubility estimates and to confirm our results.

Acknowledgments

Prasad Kasibhatla is thanked for fruitful discussions. Model outputs used in this study are freely available and can be obtained upon request from the authors. This research was supported by the National Center for Atmospheric Research, which is operated by the University Corporation for Atmospheric Research on behalf of the National Science Foundation, and by the DOE grant DE-SC0006711. We would like to acknowledge high-performance computing support from Yellowstone provided by NCAR's Computational and Information Systems Laboratory.

The Editor thanks two anonymous reviewers for their assistance in evaluating this paper.

References

Aumont, B., S. Szopa, and S. Madronich (2005), Modeling the evolution of organic carbon during its gas-phase tropospheric oxidation: Development of an explicit model based on a self generating approach, *Atmos. Chem. Phys.*, *5*, 2497–2517.

Aumont, B., R. Valorso, C. Mouchel-Vallon, M. Camredon, J. Lee-Taylor, and S. Madronich (2012), Modeling SOA formation from the oxidation of intermediate volatility *n*-alkanes, *Atmos. Chem. Phys.*, *12*, 7577–7589.

Bessagnet, B., C. Seigneur, and L. Menut (2010), Impact of dry deposition of semi-volatile organic compounds on secondary organic aerosols, *Atmos. Environ.*, *14*, 1781–1787.

Carter, W. P. L. (2010), Development of a condensed SAPRC-07 chemical mechanism, *Atmos. Environ.*, *44*, 5336–5345.

Compernolle, S., and J.-F. Müller (2014), Henry's law constants of polyols, *Atmos. Chem. Phys. Discuss.*, *14*, 13,529–13,559, doi:10.5194/acpd-14-13529-2014.

Couvidat, F., and C. Seigneur (2011), Modeling secondary organic aerosol formation from isoprene oxidation under dry and humid conditions, *Atmos. Chem. Phys.*, *11*, 893–909, doi:10.5194/acp-11-893-2011.

Donahue, N. M., A. L. Robinson, C. O. Stanier, and S. N. Pandis (2006), Coupled partitioning, dilution, and chemical aging of semivolatile organics, *Environ. Sci. Technol.*, *40*, 2635–2643, doi:10.1021/es052297c.

Emmons, L. K., et al. (2010), Description and evaluation of the Model for Ozone and Related chemical Tracers, version 4 (MOZART-4), *Geosci. Model Dev.*, *3*(1), 43–67.

Ervens, B., B. J. Turpin, and R. J. Weber (2011), Secondary organic aerosol formation in cloud droplets and aqueous particles (aqSOA): A review of laboratory, field and model studies, *Atmos. Chem. Phys.*, *11*, 11,069–11,102, doi:10.5194/acp-11-11069-2011.

Fann, N., A. D. Lamson, S. C. Anenberg, K. Wesson, D. Risley, and B. J. Hubbell (2012), Estimating the national public health burden associated with exposure to ambient $PM_{2.5}$ and ozone, *Risk Anal.*, *32*, 81–95.

Grell, G. A., and D. Dévényi (2002), A generalized approach to parameterizing convection combining ensemble and data assimilation techniques, *Geophys. Res. Lett.*, *29*(14), 1693, doi:10.1029/2002GL015311.

Hallquist, M., et al. (2009), The formation, properties and impact of secondary organic aerosol: Current and emerging issues, *Atmos. Chem. Phys.*, *9*, 5155–5235.

Hilal, S. H., S. N. Ayyampalayam, and L. A. Carreira (2008), Air-liquid partition coefficient for a diverse set of organic compounds: Henry's law constant in water and hexadecane, *Environ. Sci. Technol.*, *42*(24), 9231–9236.

Hodzic, A., J. L. Jimenez, S. Madronich, M. R. Canagaratna, P. F. DeCarlo, L. Kleinman, and J. Fast (2010), Modeling organic aerosols in a megacity: Potential contribution of semi-volatile and intermediate volatility primary organic compounds to secondary organic aerosol formation, *Atmos. Chem. Phys.*, *10*, 5491–5514, doi:10.5194/acp-10-5491-2010.

Hodzic, A., S. Madronich, B. Aumont, J. Lee-Taylor, T. Karl, M. Camredon, and C. Mouchel-Vallon (2013), Limited influence of dry deposition of semi-volatile organic vapors on secondary organic aerosol formation in the urban plume, *Geophys. Res. Lett.*, *40*, 3302–3307, doi:10.1002/grl.50611.

Jo, D. S., R. J. Park, M. J. Kim, and D. V. Spracklen (2013), Effects of chemical aging on global secondary organic aerosol using the volatility basis set approach, *Atmos. Environ.*, *81*, 230–244.

Kanakidou, M., et al. (2005), Organic aerosol and global climate modelling: A review, *Atmos. Chem. Phys.*, *5*, 1053–1123.

Karl, T., P. Harley, L. Emmons, B. Thornton, A. Guenther, C. Basu, A. Turnipseed, and K. Jardine (2010), Efficient atmospheric cleansing of oxidized organic trace gases by vegetation, *Science*, *330*(6005), 816–819, doi:10.1126/science.1192534.

Knote, C., et al. (2014a), Simulation of semi-explicit mechanisms of SOA formation from glyoxal in aerosol in a 3-D model, *Atmos. Chem. Phys.*, *14*, 6213–6239, doi:10.5194/acp-14-6213-2014.

Knote, C., A. Hodzic, and J. L. Jimenez (2014b), The effect of dry and wet deposition of condensable vapors on secondary organic aerosols concentrations over the continental US, *Atmos. Chem. Phys. Discuss.*, *14*, 13,731–13,767, doi:10.5194/acpd-14-13731-2014.

Lane, T. E., N. M. Donahue, and S. N. Pandis (2008), Simulating secondary organic aerosol formation using the volatility basis-set approach in a chemical transport model, *Atmos. Environ.*, *42*, 7439–7451.

Meylan, W. M., and P. H. Howard (2000), SRC's EPI suite, v3.20, Syracuse Research Corporation, Syracuse, N. Y.

Mouchel-Vallon, C., P. Brauer, M. Camredon, R. Valorso, S. Madronich, H. Herrmann, and B. Aumont (2013), Explicit modeling of volatile organic compounds partitioning in the atmospheric aqueous phase, *Atmos. Chem. Phys.*, *13*, 1023–1037, doi:10.5194/acp-13-1023-2013.

Murphy, B. N., and S. N. Pandis (2009), Simulating the formation of semivolatile primary and secondary organic aerosol in a regional chemical transport model, *Environ. Sci. Technol.*, *43*(13), 4722–4728, doi:10.1021/es803168a.

Myrdal, P. B., and S. H. Yalkowsky (1997), Estimating pure component vapor pressures of complex organic molecules, *Ind. Eng. Chem. Res.*, *36*, 2494–2499.

Nannoolal, Y., J. Rarey, and D. Ramjugernath (2008), Estimation of pure component properties: Part 3. Estimation of the vapor pressure of non-electrolyte organic compounds via group contributions and group interactions, *Fluid Phase Equil.*, *269*(1–2), 117–133.

Neu, J. L., and M. J. Prather (2012), Toward a more physical representation of precipitation scavenging in global chemistry models: Cloud overlap and ice physics and their impact on tropospheric ozone, *Atmos. Chem. Phys.*, *12*, 3289–3310, doi:10.5194/acp-12-3289-2012.

Pankow, J. F. (1994), An absorption-model of the gas aerosol partitioning involved in the formation of secondary organic aerosol, *Atmos. Environ.*, *28*, 189–193.

Pye, H. O. T., and J. H. Seinfeld (2010), A global perspective on aerosol from low-volatility organic compounds, *Atmos. Chem. Phys.*, *10*, 4377–4401, doi:10.5194/acp-10-4377-2010.

Pye, H. O. T., et al. (2010), Global modeling of organic aerosol: The importance of reactive nitrogen (NO_x and NO_3), *Atmos. Chem. Phys.*, *10*, 11,261–11,276, doi:10.5194/acp-10-11261-2010.

Raventos-Duran, T., M. Camredon, R. Valorso, C. Mouchel-Vallon, and B. Aumont (2010), Structure-activity relationships to estimate the effective Henry's law constants of organics of atmospheric interest, *Atmos. Chem. Phys.*, *10*, 7643–7654, doi:10.5194/acp-10-7643-2010.

Robinson, A. L., N. M. Donahue, M. K. Shrivastava, E. A. Weitkamp, A. M. Sage, A. P. Grieshop, T. E. Lane, S. N. Pandis, and J. R. Pierce (2007), Rethinking organic aerosols: Semivolatile emissions and photochemical aging, *Science*, *315*, 1259–1262.

Seinfeld, J. H., and S. N. Pandis (2006), *Atmospheric Chemistry and Physics: From Air Pollution to Climate Change*, 2nd ed., John Wiley, Hoboken, N. J.

Tolocka, M. P., M. Jang, J. M. Ginter, F. J. Cox, R. M. Kamens, and M. V. Johnston (2004), Formation of oligomers in secondary organic aerosol, *Environ. Sci. Technol.*, *38*(5), 1428–1434, doi:10.1021/es035030r.

Vaden, T. D., D. Imre, J. Beranek, M. Shrivastava, and A. Zelenyuk (2011), Evaporation kinetics and phase of laboratory and ambient secondary organic aerosol, *Proc. Natl. Acad. Sci. U.S.A.*, *108*, 2190–2195, doi:10.1073/pnas.1013391108.

Wesely, M. L. (1989), Parameterizations of surface resistance to gaseous dry deposition in regional-scale, numerical models, *Atmos. Environ.*, *23*, 1293–1304.

Zaveri, R. A., R. C. Easter, J. D. Fast, and L. K. Peters (2008), Model for simulating aerosol interactions and chemistry (MOSAIC), *J. Geophys. Res.*, *113*, D13204, doi:10.1029/2007JD008782.

Zhang, Q., et al. (2007), Ubiquity and dominance of oxygenated species in organic aerosols in anthropogenically-influenced Northern Hemisphere midlatitudes, *Geophys. Res. Lett.*, *34*, L13801, doi:10.1029/2007GL029979.